NEURAL REGENERATION RESEARCH
April 2014, Volume 9, Issue 8
www.nrronline.org

Regulatory effects of anandamide on intracellular Ca^{2+} concentration increase in trigeminal ganglion neurons

Yi Zhang[1], Hong Xie[2], Gang Lei[3], Fen Li[3], Jianping Pan[3], Changjin Liu[3], Zhiguo Liu[4], Lieju Liu[4], Xuehong Cao[3, 4]

1 Department of Anesthesiology, Tongji Hospital Affiliated to Tongji Medical College, Huazhong University of Science and Technology, Wuhan, Hubei Province, China
2 Jingzhou Central Hospital, Jingzhou, Hubei Province, China
3 Department of Physiology, Tongji Medical College, Huazhong University of Science and Technology, Wuhan, Hubei Province, China
4 Department of Bioengineering, Wuhan Institute of Engineering, Wuhan, Hubei Province, China

Corresponding author:
Xuehong Cao, M.D., Ph.D., Department of Physiology, Tongji Medical College, Huazhong University of Science and Technology, Wuhan 430030, Hubei Province, China; Department of Bioengineering, Wuhan Institute of Engineering, Wuhan 430023, Hubei Province, China, caoxuehong@gmail.com.
Lieju Liu, M.D., Department of Bioengineering, Wuhan Institute of Engineering, Wuhan 430023, Hubei Province, China, liejuliu@gmail.com.

doi:*10.4103/1673-5374.131607*
http:*//www.nrronline.org/*

Accepted: *2014-03-21*

Abstract

Activation of cannabinoid receptor type 1 on presynaptic neurons is postulated to suppress neurotransmission by decreasing Ca^{2+} influx through high voltage-gated Ca^{2+} channels. However, recent studies suggest that cannabinoids which activate cannabinoid receptor type 1 can increase neurotransmitter release by enhancing Ca^{2+} influx *in vitro*. The aim of the present study was to investigate the modulation of intracellular Ca^{2+} concentration by the cannabinoid receptor type 1 agonist anandamide, and its underlying mechanisms. Using whole cell voltage-clamp and calcium imaging in cultured trigeminal ganglion neurons, we found that anandamide directly caused Ca^{2+} influx in a dose-dependent manner, which then triggered an increase of intracellular Ca^{2+} concentration. The cyclic adenosine and guanosine monophosphate-dependent protein kinase systems, but not the protein kinase C system, were involved in the increased intracellular Ca^{2+}concentration by anandamide. This result showed that anandamide increased intracellular Ca^{2+} concentration and inhibited high voltage-gated Ca^{2+} channels through different signal transduction pathways.

Key Words: *nerve regeneration; trigeminal ganglion; neurons; endocannabinoids; anandamide; cannabinoid receptor type 1; voltage-dependent calcium channels; vanilloid receptor; patch-clamp technique; calcium; cyclic adenosine monophosphate protein kinase; protein kinase C; NIH grant; neural regeneration*

Funding: *This work was supported by NIH, grant No. GM-63577; NNSF, grant No. 30571537, No. 30271500; the National Natural Science Foundation of China, No. 30271500, 30571537 and 81370246. 2010 National Clinical Key Disciplines Construction Grant from the Ministry of Health of the People's Republic of China.*

Zhang Y, Xie H, Lei G, Li F, Pan JP, Liu CJ, Liu ZG, Liu LJ, Cao XH. Regulatory effects of anandamide on intracellular Ca^{2+} concentration increase in trigeminal ganglion neurons. Neural Regen Res. 2014;9(8):878-887.

Introduction

N-arachidonoylethanolamine (anandamide) is referred to as the first 'endocannabinoid' described, and anandamide signaling has been reported to be an inhibitor of axon regeneration. Anandamide acts primarily on cannabinoid receptor type 1 (CB_1)[1], cannabinoid receptor type 2 (CB_2)[2], and ionotropic receptors, including the transient receptor potential (TRP) vanilloid type 1 (TRPV1)[3-5], TRP ankyrin type 1 (TRPA1) and TRP melastatin type 8 (TRPM8) channels[6]. Anandamide can also directly modulate various other ion channels[5, 7-10].

CB_1 and CB_2 are members of the subfamily of G-protein-coupled receptors and predominantly couple to Gi/o[1, 11] to produce multiple cellular effects, such as the inhibition of adenylate cyclase and of voltage-gated calcium channels[12-14], regulation of potassium currents[15-17], and increase of Ca^{2+} influx *via* G_s[18] and G_q[19]. TRPV1 is a polymodal sensor of noxious stimuli including heat, hydrogen ions and capsaicin[20]. CB_1[21] and TRPV1, but not CB_2[21] are expressed in presynaptic primary neurons such as those in the trigeminal ganglion. CB_1 is localized to presynaptic nerve terminals[22] and contributes to the regulation of neuronal excitability and neurotransmitter release by modulating Ca^{2+} signals. TRPV1 activation causes Ca^{2+} to enter into the cell and promotes neurotransmitter release. Studies have demonstrated that anandamide can activate TRPV1 by binding to cytosolic sites[23]. The co-expression and close distribution of CB_1 and TRPV1 in primary sensory neurons[24-27] allows cross-talk between these two receptors, which further complicates the role of anandamide in nociception and antinociception. The present study will determine which receptor contributes to the effect of low and high concentrations of anandamide in small trigeminal ganglion neurons.

It is a widely accepted general hypothesis that endocannabinoids inhibit neurotransmitter release from primary afferent neurons by reducing Ca^{2+} influx *via* an inhibitory action on high voltage-gated Ca^{2+} channels. This hypothesis is supported by evidence that CB_1 activation by anandamide

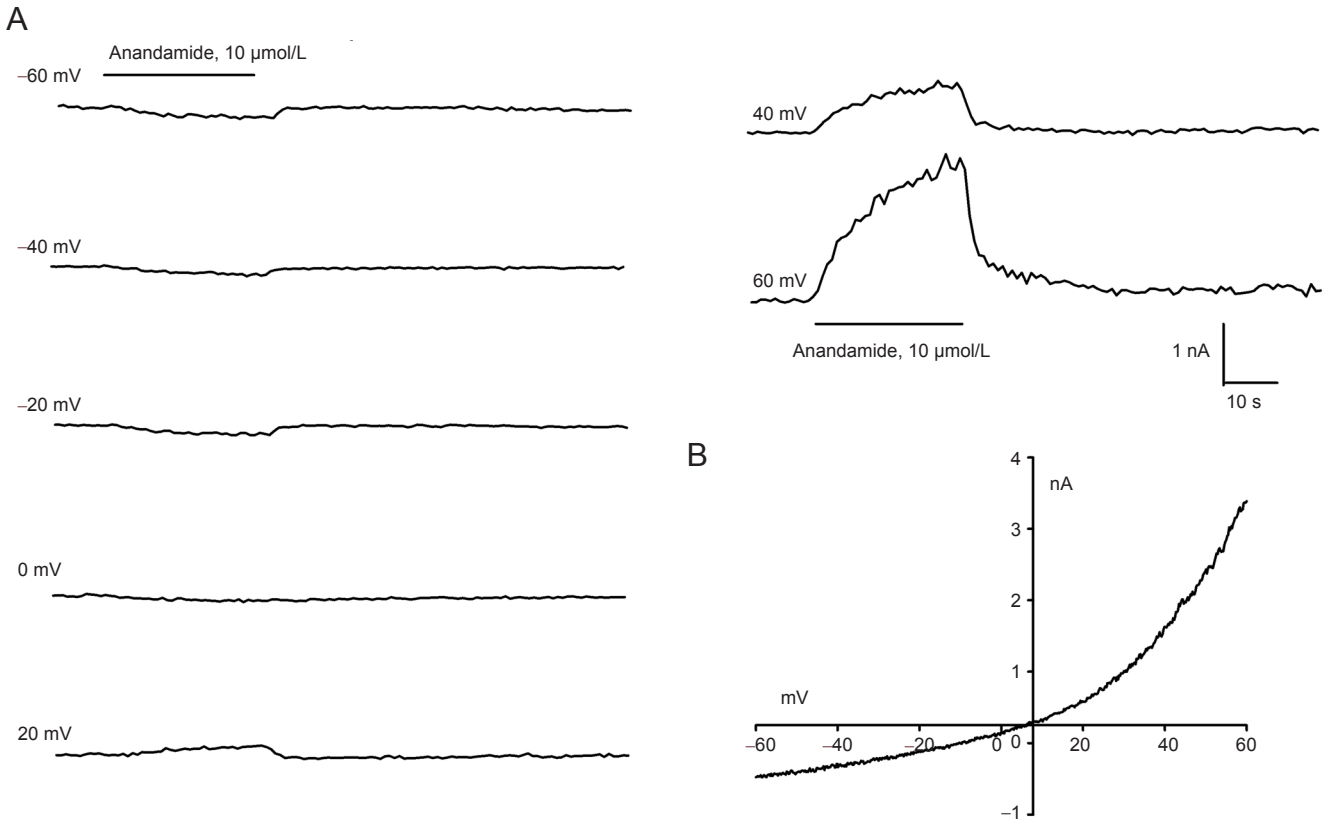

Figure 1 Anandamide-evoked currents in rat trigeminal ganglion neurons.
(A) Typical traces of 10 μmol/L anandamide-induced currents at different holding potentials (−60 to 60 mV) applied to a neuron. Bar indicates duration of stimulus. (B) Current-voltage relationship of 10 μmol/L anandamide-induced currents at different holding potentials. s: Second.

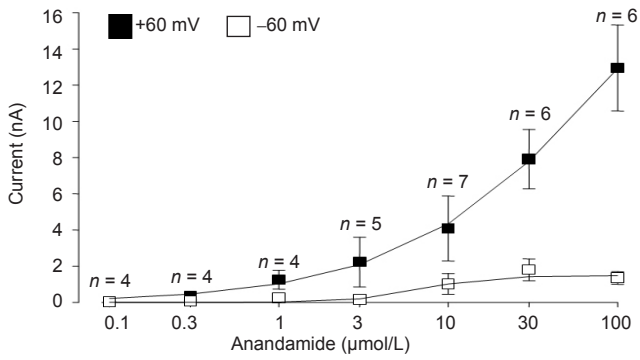

Figure 2 Dose-dependent anandamide-evoked currents (nA) in trigeminal ganglion neurons, measured by the voltage-ramp method from −60 to +60 mV.
n numbers represent individual experiments for each data point.

on primary nociceptive neurons causes antinociception by reducing high voltage-activated Ca^{2+} channel activity[12-14] and Ca^{2+} influx[28], thus inhibiting neurotransmission. In contrast, some studies suggest that cannabinoids can promote Ca^{2+} influx and hence increase neurotransmitter release *in vitro*[19, 25, 29-31]. How endocannabinoids may cause such opposing effects in intracellular Ca^{2+} concentration and neuron excitability is unclear. High voltage-gated calcium channels and ligand-gated channels, two important contributors to intracellular Ca^{2+} concentration, will also be investigated. The present study tests the above hypothesis by determining the effect of anandamide on high voltage-activated Ba^{2+} currents (I_{HVA}), Ca^{2+} influx and intracellular Ca^{2+} concentration, as well as the underlying mechanisms, in small trigeminal ganglion neurons.

Results

Anandamide-evoked inward currents

Whole-cell patch-clamp recordings were carried out in rat trigeminal ganglion neurons with bath perfusion of 0.1, 0.3, 1, 3, 10, 30 and 100 μmol/L anandamide at a range of holding potentials from −60 mV to +60 mV (Figure 1). Reversal potentials were around 0 mV. Anandamide-evoked inward and outward currents at holding potentials of −60 mV and +60 mV, respectively, were dose-dependent (Figure 2).

Inhibition of I_{HVA} by anandamide

Bath application of anandamide (0.001, 0.01, 0.1, 1, 10, 30 μmol/L) inhibited I_{HVA} in a concentration-dependent manner, by 4.62 ± 0.88%, 6.24 ± 2.57%, 18.17 ± 0.99%, 31.30 ± 3.21%, 64.73 ± 1.95% and 55.19 ± 2.06%, respectively (n = 4–11). The effect of anandamide was partially reversed after washout. The Hill equation was applied to the dose-response curve and revealed that the half-maximal inhibitory concentration (IC_{50}) of anandamide was 0.92 μmol/L. To confirm whether other CB_1 agonists mimicked the inhibition of anandamide, we tested the effect of WIN 55,212-2 (10 μmol/L) on I_{HVA}. The inhibition of I_{HVA} by 10 μmol/L WIN 55,212-2 was 55.78 ± 6.07%. Anandamide at 1 μmol/L reduced current amplitudes (Figure 3A, B) but did not cause a significant shift of the activation curve (Figure 3C). However, a hyperpolarization shift of almost 14 mV (n = 8; $P < 0.05$) was ob-

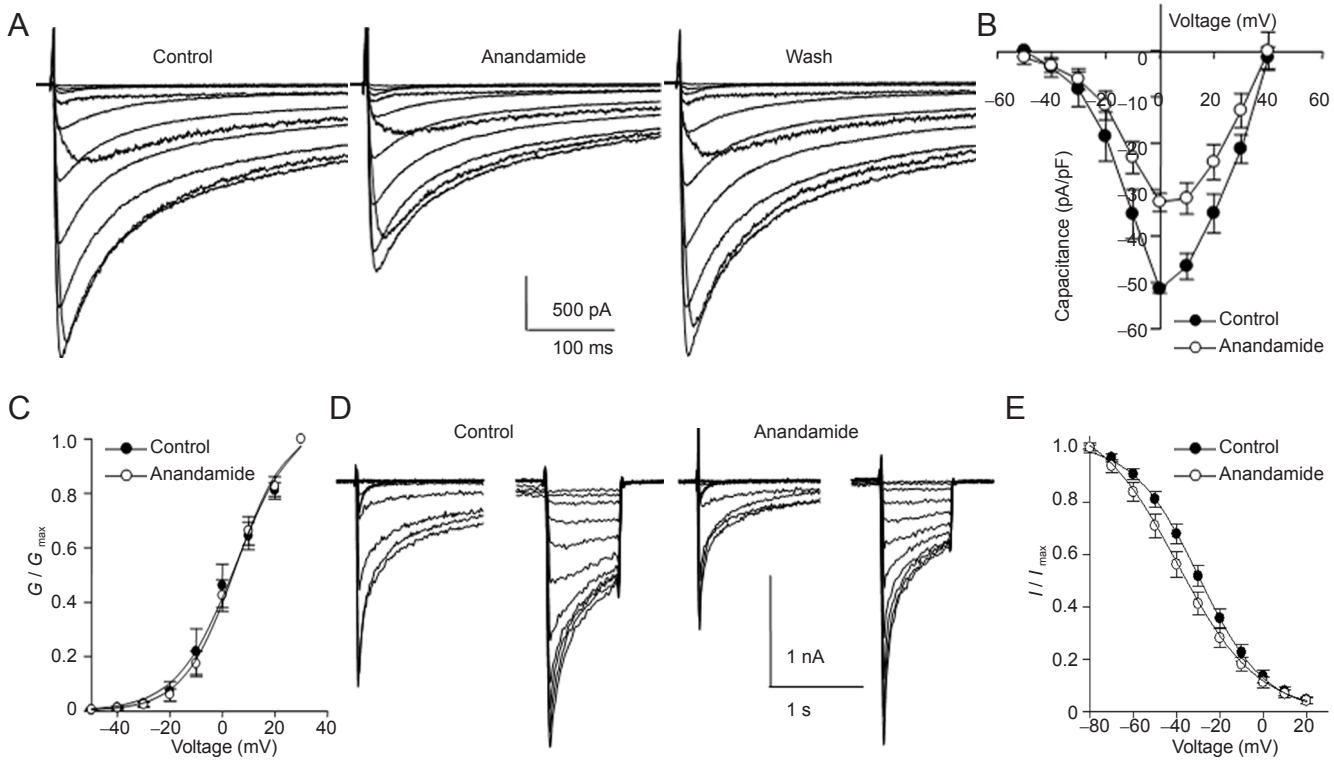

Figure 3 Inhibition of high voltage-activated Ca^{2+} currents (I_{HVA}) in rat trigeminal ganglion neurons by exposure to anandamide (1 μmol/L) for 3 minutes.

(A) I_{HVA} reduced from −2.42 nA to −1.67 nA, returning to −2.29 nA after 3 minutes of washout. Traces were evoked by 450 ms step depolarization from −50 mV to 40 mV in 10 mV increments. (B) Current-voltage curve of I_{HVA}. Anandamide perfusion for 3 minutes reduced the peak current intensity of I_{HVA} from −51.50 ± 0.85 pA/pF to −32.73 ± 1.97 pA/pF (mean ± SEM, n = 8; paired t-test, anandamide, *vs.* control, $P < 0.001$). (C) As the amplitude of I_{HVA} reduced, the activation curve was not affected. The Boltzmann function was fitted to the activation curve. Before and after 1 μmol/L anandamide application, $V_{0.5}$ values were −3.73 ± 4.36 mV and −6.47 ± 3.02 mV, respectively (n = 7, paired t-test, $P > 0.05$), and k values (slope) were 8.74 ± 0.75 and 10.10 ± 0.58, respectively (n = 7, paired t-test, $P > 0.05$). (D) Effect of 1 μmol/L anandamide on the h-infinity curve. The steady-state inactivation-voltage protocol consisted of 3 seconds of preconditioned pulses ranging from −80 mV to 20 mV followed by a 200 ms test pulse depolarizing to 20 mV. (E) Anandamide hyperpolarization shifted the h-infinity curve. After fitting the Boltzmann function, $V_{0.5}$ values were −30.93 ± 2.75 mV and −45.32 ± 5.61 mV (n = 8, paired t-test, $P < 0.05$), and k values were −15.78 ± 1.33 and −15.85 ± 2.58 (n = 8, paired t-test, $P > 0.05$) before and after anandamide administration. s: Second.

served in the h-infinity curve (Figure 3E).

Roles of cannabinoid and vanilloid receptors in the inhibition of I_{HVA} by anandamide

Since anandamide activates TRPV1, CB_1 and CB_2 receptors, we tested whether capsazepine, AM251 and AM630, selective antagonists at the three receptors, respectively, could reverse the effect of anandamide on I_{HVA}. Capsazepine (10 μmol/L), AM251 (10 μmol/L), AM630 (10 μmol/L), or anandamide (1 and 10 μmol/L) were added to the bath solution during whole-cell patch clamp recordings in rat trigeminal ganglion neurons. First, we examined how pre-incubation of the cells for 3 minutes with capsazepine, a competitive antagonist at TRPV1, would affect the inhibition induced by anandamide (Figure 4A, D). Pre-incubation with capsazepine did not affect the inhibition of I_{HVA} by 1 μmol/L anandamide (n = 10, $P > 0.05$), but abolished the effect of 10 μmol/L anandamide (n = 12, $P < 0.05$). These data indicate that TRPV1 activation is involved in the inhibition of I_{HVA} by high-concentration anandamide. AM251 was co-applied with anandamide (1 or 10 μmol/L) (Figure 4B, E). Low-dose (n = 7, $P < 0.05$) and high-dose (n = 4, $P < 0.05$) anandamide-induced inhibition was reversed by AM251 (Figure 4G), indicating that activation of CB_1 is essential for the negative modulation of I_{HVA} by anandamide in rat trigeminal ganglion neurons.

Pre-incubation for 3 minutes with AM630 did not affect I_{HVA} inhibition induced by 1 μmol/L (Figure 4C, G; $P > 0.05$) or 10 μmol/L (Figure 4F, G; $P > 0.05$) anandamide, indicating a lack of CB2 receptors in rat trigeminal ganglion neurons[21].

Inhibition of I_{HVA} by capsaicin

As described above, inhibition of I_{HVA} by high-concentration anandamide was reversed by the TRPV1 antagonist capsazepine, suggesting that TRPV1 is involved in this effect. We further tested whether I_{HVA} could be directly inhibited by the TRPV1 agonist, capsaicin. Capsaicin and capsazepine were applied by bath perfusion. I_{HVA} was reversibly inhibited by capsaicin in a dose-dependent manner (Figure 5). Similar to the effect observed with high-concentration anandamide, the decrease in I_{HVA} by capsaicin was reversed by 10 μmol/L capsazepine. In addition, I_{HVA} was not inhibited by 10 μmol/L capsazepine (Figure 6).

Characterization of signal transduction pathways mediating the inhibition of I_{HVA} *via* cannabinoid type-1 receptor activation by low-concentration anandamide

Three important signal transduction systems were examined using specific agonists and antagonists to test whether these

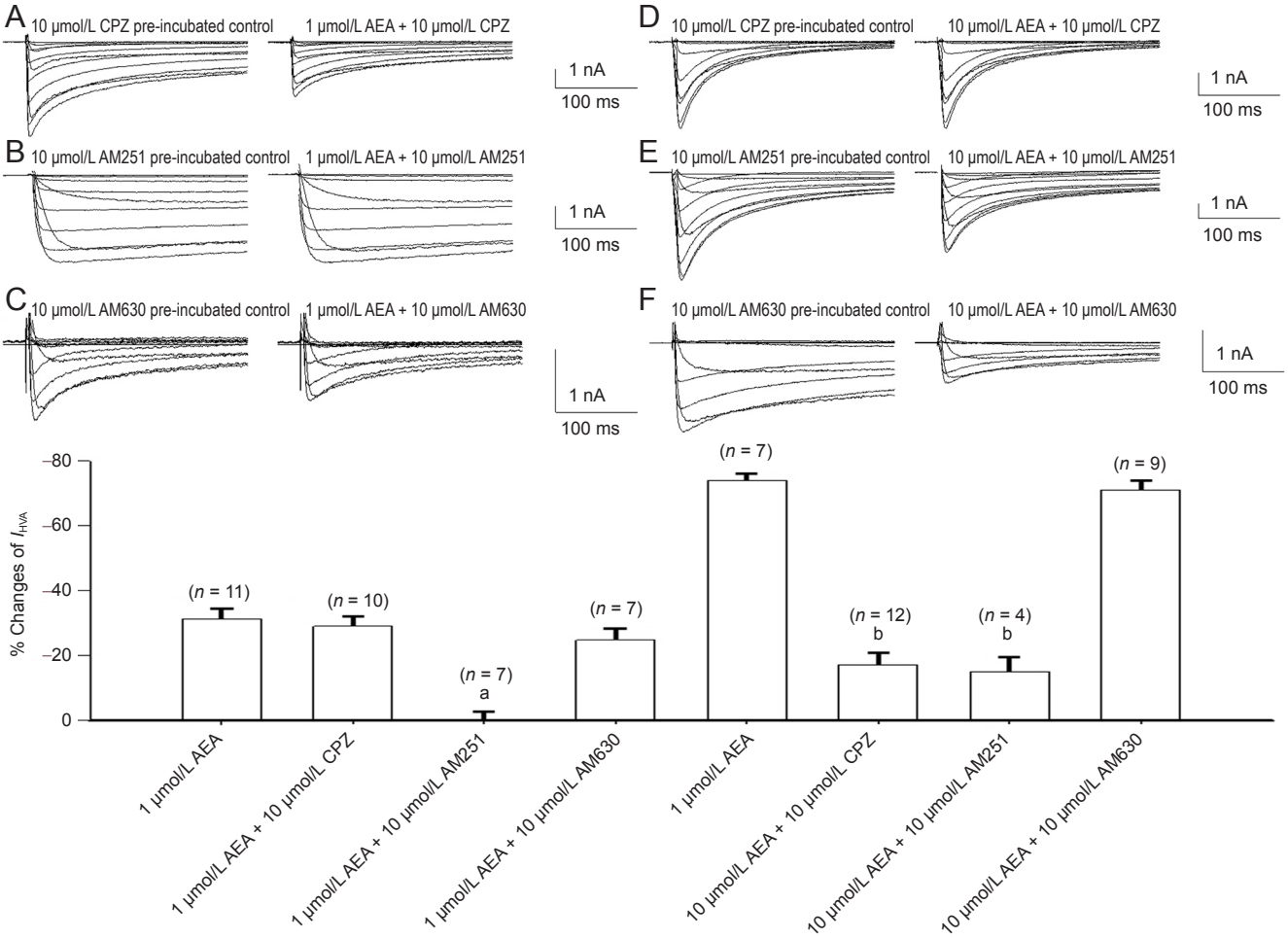

Figure 4 Cannabinoid and TRPV1 receptor involvement in the inhibition of high voltage-activated Ba^{2+} currents (I_{HVA}) by 1 and 10 μmol/L anandamide in rat trigeminal ganglion neurons.

Pre-incubation with capsazepine (A) or AM630 (C) did not affect I_{HVA} inhibition by 1 μmol/L anandamide. (B) Pre-incubation with AM251 abolished I_{HVA} inhibition by 1 μmol/L anandamide. The decrease in I_{HVA} induced by 10 μmol/L anandamide was partially attenuated by pre-infusion with capsazepine (D) or AM251 (E). Pre-incubation with AM630 (F) had no effect on 10 μmol/L anandamide-induced inhibition of I_{HVA}. (G) Summary data of the effect of cannabinoid and TRPV1 receptor antagonists on the inhibition of I_{HVA} by 1 and 10 μmol/L anandamide. $^aP < 0.01$, *vs.* inhibition induced by 1 μmol/L anandamide (unpaired Student's *t*-test). $^bP < 0.01$, *vs.* inhibition induced by 10 μmol/L anandamide (unpaired Student's *t*-test). Data are expressed as mean ± SEM. *n*: number of neurons tested. CPZ: Capsazepine; AEA: anandamide.

systems participated in the inhibition of I_{HVA} by CB1 receptors activated by 1 μmol/L anandamide.

Whole-cell patch clamp measurements in trigeminal ganglion neurons revealed that application of 1 μmol/L KT5720, an inhibitor of cyclic adenosine monophosphate -dependent protein kinase A, significantly attenuated the inhibition of I_{HVA} by 1 μmol/L anandamide (Figure 7). Incubation with an antagonist of protein kinase C, bisindolylmaleimide (1 μmol/L for 10 minutes) and an inhibitor of cyclic guanosine monophosphate (cGMP)-dependent protein kinase, Rp-8-Br-cGMP (1 μmol/L for 10 minutes) also significantly attenuated anandamide-induced inhibition of I_{HVA}.

Anandamide increased intracellular Ca^{2+} concentration *via* a direct influx of extracellular calcium into rat trigeminal ganglion neurons

Calcium imaging was used to examine the effect of anandamide on intracellular Ca^{2+} concentration in the presence of solutions containing either 0 or 2 mmol/L Ca^{2+} (Figure 8A). In the absence of extracellular calcium (buffered by 10 mmol/L ethylene glycol bis(alpha-aminoethyl ether)-N,N′-tetraacetic acid to decrease extracellular Ca^{2+} concentrations), the rise in intracellular Ca^{2+} concentration induced by anandamide was notably decreased (Figure 8B; anandamide$_{([Ca^{2+}]_+)}$: 20.33 ± 2.10%, n = 19; anandamide($[Ca^{2+}]_-$): 4.22 ± 1.06%, n = 48; $P < 0.01$). Thus, the anandamide-induced rise in intracellular Ca^{2+} concentration is dependent on Ca^{2+} influx from the extracellular space.

Cannabinoid / vanilloid type-1 receptor involvement in the mechanism underlying increased intracellular Ca^{2+} concentration evoked by anandamide

Because AM630 had no effect on the inhibition of anandamide on I_{HVA}, in the present test only AM251 and capsazepine were used, to determine whether they would affect the increase of anandamide on the intracellular Ca^{2+} concentration, using calcium imaging. The 1 μmol/L anandamide-induced rise in intracellular Ca^{2+} concentration was abolished by co-application with 10 μmol/L AM251 (Figure 8C), while lower doses of AM251 (1 and 3 μmol/L) facilitated the in-

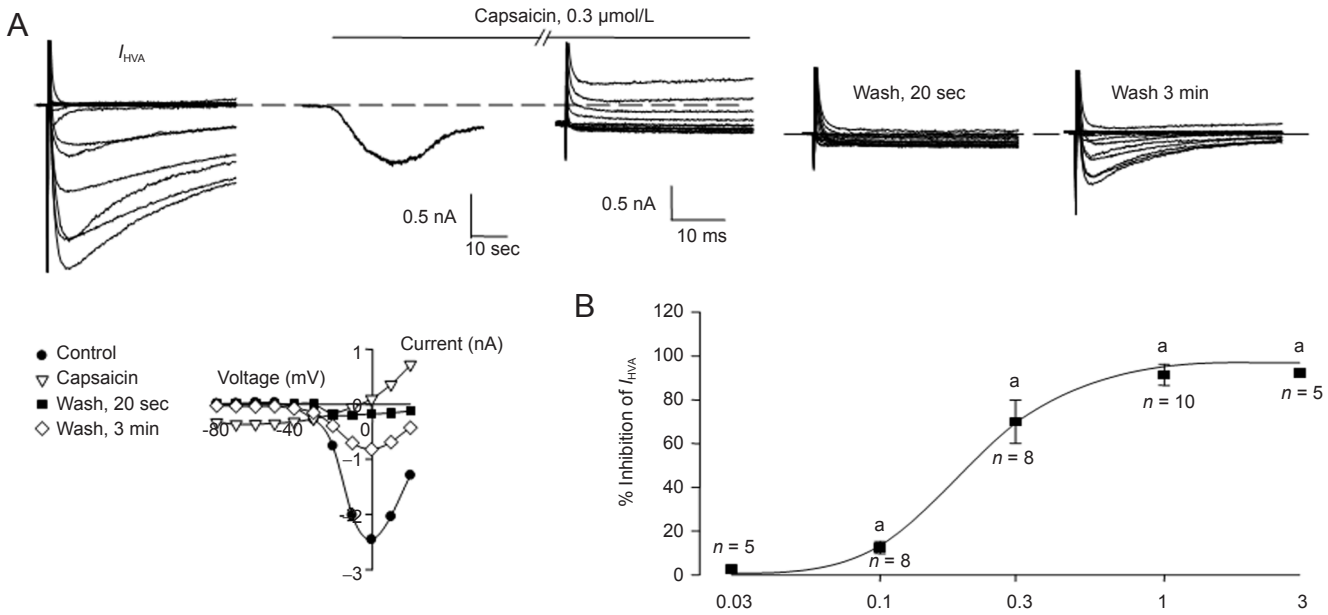

Figure 5 Cannabinoid and transient receptor potential (TRP) vanilloid type 1 receptor involvement in the inhibition of high voltage-activated Ca^{2+} currents (I_{HVA}) by 1 and 10 μmol/L anandamide in rat trigeminal ganglion neurons.
(A) I_{HVA} currents were generated in a neuron with a membrane resistance of 878 MΩ. Application of 0.3 μmol/L capsaicin induced a maximum inward current of 0.6 nA, which desensitized to 0.3 nA after about 60 seconds (sec). At this time, the membrane resistance was 164 MΩ and I_{HVA} was reduced from 2.4 to 0.4 nA. After washing the cell for 20 seconds (sec), the capsaicin-induced inward current returned to baseline and the membrane resistance increased to 856 MΩ. I_{HVA} recovered to 0.8 nA. Current-voltage curves are shown in the absence and presence of capsaicin as well as for the 20 sec and 3-minute (min) washes. (B) Dose-dependent inhibition of I_{HVA} by capsaicin in capsaicin-sensitive trigeminal ganglion neurons. The Hill equation was fitted to the dose-response curve, with IC_{50} = 0.21 μmol/L. *n*: Times of individual experiments carried out at each concentration. $^aP < 0.05$, *vs.* before capsaicin (one-way analysis of variance).

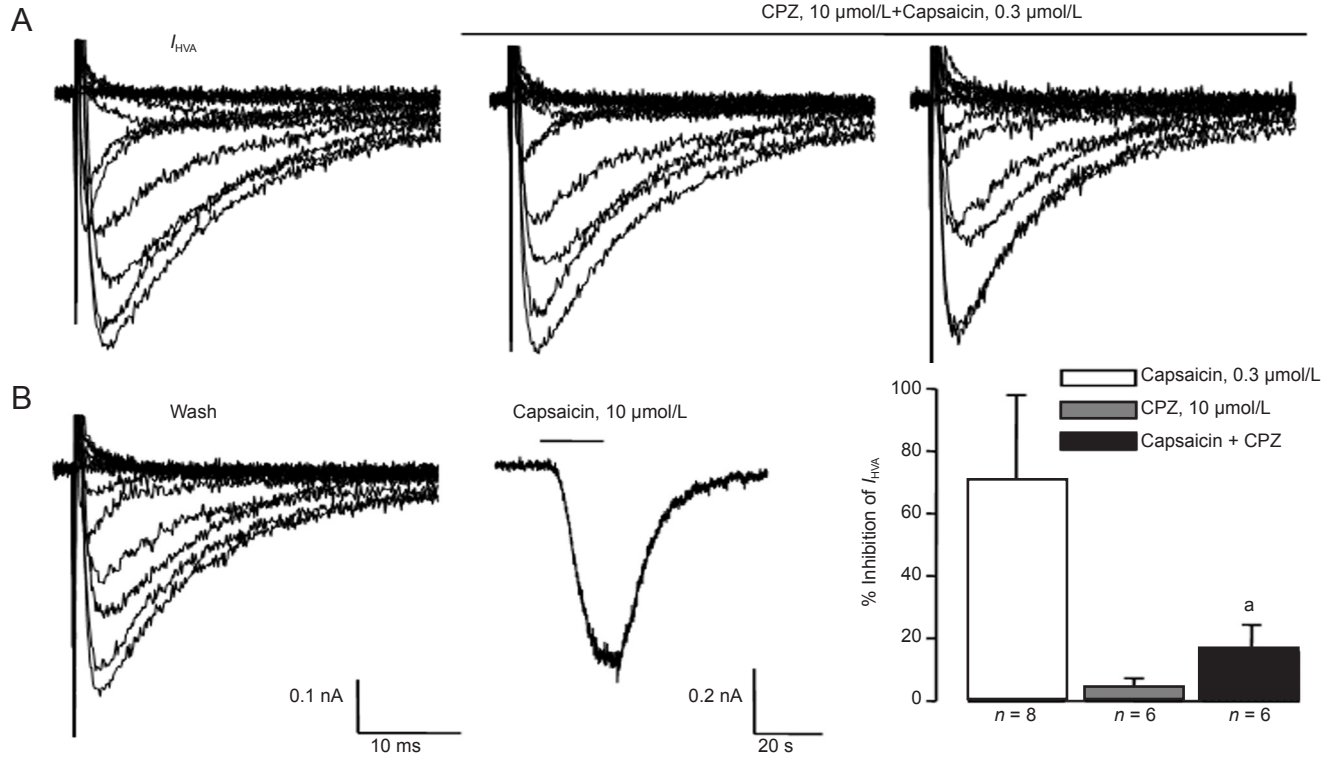

Figure 6 Capsazepine (CPZ) inhibited the capsaicin-induced decrease of Ca^{2+} current (I_{HVA}) in trigeminal ganglion neurons.
(A) Representative traces showing the effects of co-application of capsazepine and capsaicin in a capsaicin-sensitive neuron. (B) Summary data of capsazepine blockade of capsaicin-induced inhibition of I_{HVA}. $^aP < 0.01$, *vs.* capsaicin alone by unpaired *t*-test. "*n*" indicate the times of neurons tested. After I_{HVA} was obtained, neurons were incubated for 3 minutes (min) with 10 μmol/L capsazepine. Capsazepine did not affect the I_{HVA}. With a subsequent application of 0.3 μmol/L capsaicin plus 10 μmol/L capsazepine, and after a 3-minute wash, I_{HVA} remained unchanged. An inward current was induced by 10 μmol/L capsaicin, suggesting it was a capsaicin-sensitive neuron. On average, in the presence of 0.3 μmol/L capsaicin, I_{HVA} was inhibited by 70.0 ± 9.9% (n = 8). In the presence of 10 μmol/L capsazepine, I_{HVA} was inhibited by 2.8 ± 1.8% (n = 6). In the presence of 0.3 μmol/L capsaicin plus 10 μmol/L capsazepine, the inhibition of capsaicin was reduced to 15.5 ± 8.9% ($P < 0.01$). s: Second.

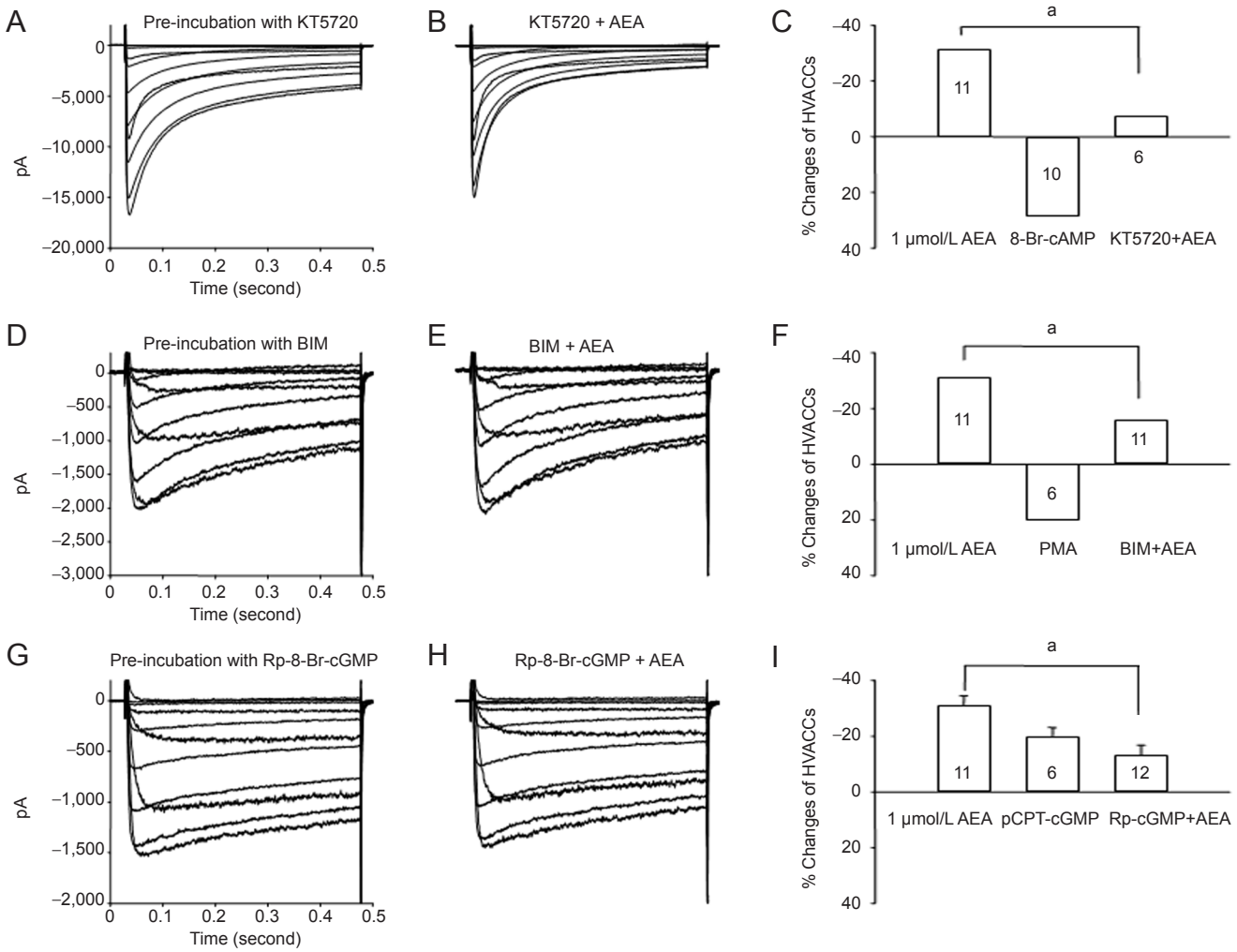

Figure 7 The role of different signaling pathways in the inhibition of 1 μmol/L anandamide on Ca^{2+} currents (I_{HVA}) in rat trigeminal ganglion neurons.
Sample traces of I_{HVA} currents pre-treated with KT5720 (1 μmol/L for 10 minutes in the bath solution) (A) and responding to co-application with 1 μmol/L anandamide for 3 minutes (B). (C) Averaged effects of 8-Br-cAMP alone and KT5720 co-application with 1 μmol/L anandamide on I_{HVA}. Typical traces of I_{HVA} currents pre-treated with BIM (10 μmol/L for 10 minutes in the bath solution) (D) and responding to co-application with 1 μmol/L anandamide for 3 minutes (E, F). Typical traces of I_{HVA} currents in neurons pre-treated with Rp-8-Br-cGMP (1 μmol/L for 10 minutes in the bath solution) (G) and anandamide (1 μmol/L) for 3 minutes (H). (I) Mean (± SEM) effects on I_{HVA} of pCPT-cGMP alone and Rp-8-Br-cGMP co-application with anandamide (1 μmol/L). $^aP < 0.01$, *vs.* anandamide (unpaired *t*-test). Numbers in bars indicate the number of neurons tested. I_{HVA}: High voltage-activated Ca^{2+} currents; cGMP: cyclic guanosine monophosphate; cAMP: cyclic adenosine monophosphate; AEA: anandamide.

crease of 1 μmol/L anandamide (Figure 8C). This suggests that co-incubation with 1 μmol/L anandamide and low-dose AM251 facilitates intracellular Ca^{2+} influx *via* TRPV1 while at the same time inhibiting it *via* CB_1 receptors.

Similar to the effect of 10 μmol/L anandamide observed on I_{HVA}, the increase in intracellular Ca^{2+} concentration was also blocked by both AM251 and capsazepine (Figure 8C), indicating that different receptors participate in the responses of intracellular Ca^{2+} concentration to low and high concentrations of anandamide in rat trigeminal ganglion neurons.

Signaling pathways mediating the increase in intracellular Ca^{2+} concentration after cannabinoid receptor activation by low-concentration anandamide

Calcium imaging was used to evaluate the possible contribution of cAMP-dependent protein kinase, protein kinase C, and cGMP-dependent protein kinase systems to the observed effect on intracellular Ca^{2+} concentration after CB1 activation. The effects of 1 μmol/L anandamide on intracellular Ca^{2+} concentrations in trigeminal ganglion neurons pre-treated with KT5720 (an inhibitor of cAMP-dependent protein kinase), staurosporine (an inhibitor of protein kinase C) and KT5823 (an inhibitor of cGMP-dependent protein kinase) were investigated. Figure 8D showed that staurosporine (10 μmol/L for 15 minutes) had no effect on the rise in intracellular Ca^{2+} concentration after anandamide application ($n = 13$, $P > 0.05$). Pretreatment with KT5720 (10 μmol/L for 10 minutes) and KT5823 (10 μmol/L for 10 minutes) markedly attenuated the response of 1 μmol/L anandamide (Figure 8D). These data suggest that the cAMP-dependent protein kinase and cGMP-dependent protein kinase systems, but not the protein kinase C system, are involved in the increase in intracellular Ca^{2+} concentration with 1 μmol/L anandamide.

Discussion

It is well established that presynaptic CB_1 receptor activation

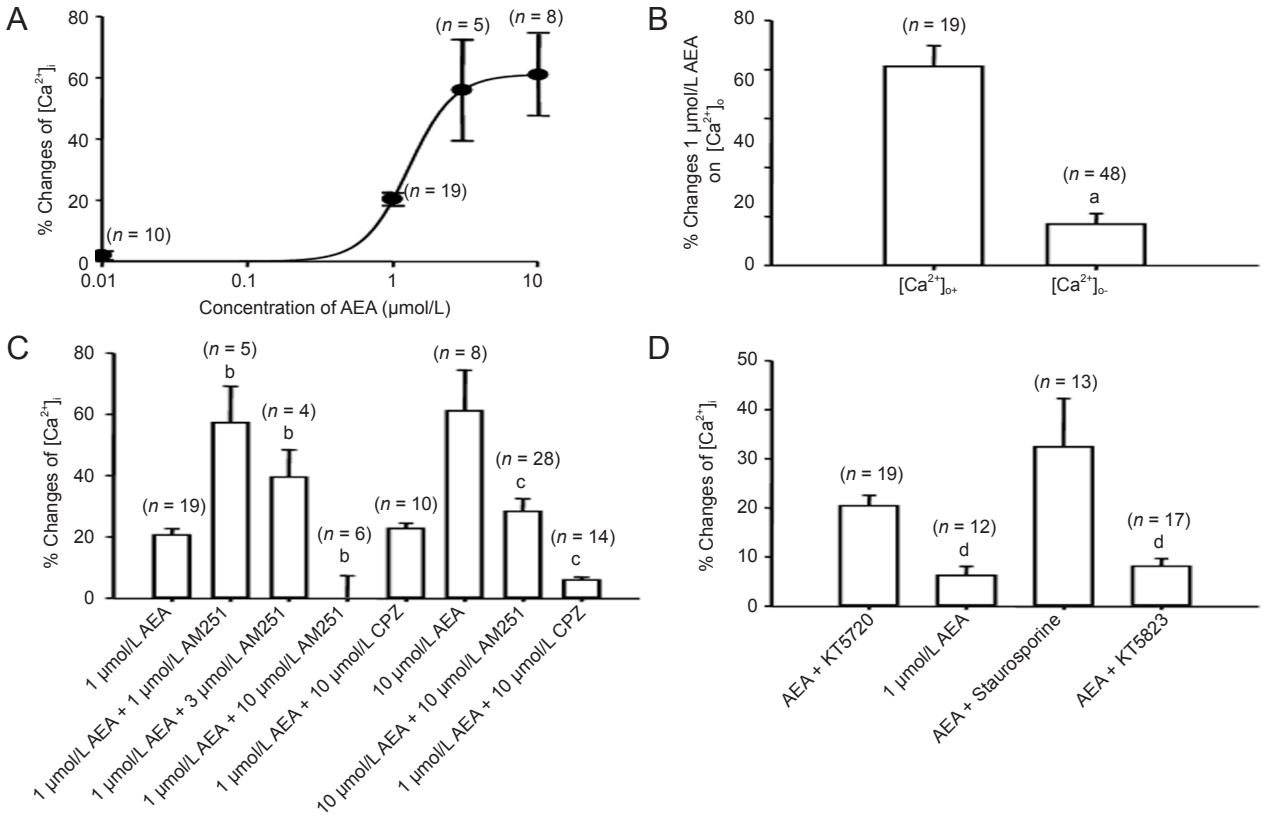

Figure 8 Effects of anandamide on intracellular Ca^{2+} concentration ($[Ca^{2+}]_i$) in rat trigeminal ganglion neurons.
(A) Concentration-response curve for increases in ($[Ca^{2+}]_i$) with anandamide application. (B) Different responses in $[Ca^{2+}]_i$ evoked by 1 μmol/L anandamide in the presence and absence of extracellular Ca^{2+} ($[Ca^{2+}]_o$). A significant effect was seen with 2 mmol/L Ca^{2+} present in the extracellular environment ($n = 19$) compared with the Ca^{2+}-free condition ($n = 48$), $^aP < 0.01$, *vs.* presence of extracellular Ca^{2+} (unpaired Student's *t*-test). (C) Responses (mean ± SEM) induced by 1 and 10 μmol/L anandamide and their co-application with AM251 and capsazepine. Pre-incubation with 10 μmol/L AM251 reversed the rises evoked by 1 and 10 μmol/L anandamide ($^bP < 0.01$, *vs.* 1 μmol/L anandamide alone; one-way analysis of variance; $^cP < 0.01$ *vs.* 10 μmol/L anandamide alone; one-way analysis of variance). 1 and 3 μmol/L AM251 facilitated the increase induced by 1 μmol/L anandamide. Pre-application of 10 μmol/L capsazepine blocked the 10 μmol/L anandamide-induced increase in intracellular Ca^{2+} concentration ($n = 14$, $^cP < 0.01$, *vs.* 10 μmol/L anandamide alone), while the increase evoked by 1 μmol/L anandamide was not affected by pre-treatment with 10 μmol/L capsazepine ($P > 0.05$, *vs.* 1 μmol/L anandamide alone). (D) Mean (±SEM) responses of preperfusion with KT5720, staurosporine and KT5823 and followed by co-application of 1 μmol/L anandamide. The rise evoked by 1 μmol/L anandamide was blocked by KT5720 ($^dP < 0.01$, *vs.* 1 μmol/L anandamide alone) and KT5823 ($^dP < 0.01$, *vs.* anandamide alone) but not staurosporine ($P > 0.05$, *vs.* anandamide alone, one-way analysis of variance). Numbers in parentheses indicate the number of neurons tested. CPZ: Capsazepine; AEA: anandamide.

has an inhibitory role on high voltage-activated Ca^{2+} channels, resulting in a decrease in Ca^{2+} influx and an inhibition of neurotransmitter release. In contrast, results from the present study show that anandamide causes a dose-dependent elevation of intracellular Ca^{2+} concentration, triggered by anandamide-evoked currents, but not modulation of high voltage-activated Ca^{2+} channels by anandamide. Furthermore, anandamide-induced inhibition of the high voltage-activated Ca^{2+} channels and the increase in the intracellular Ca^{2+} concentration are demonstrated to be two separate events differing in signal transduction pathways but having similar effects *via* the same receptors. Thus, our data suggest that anandamide, as an endocannabinoid, might exert an excitatory effect by increasing intracellular Ca^{2+} concentration, triggered by anandamide-evoked currents.

It has been well documented that the endocannabinoid anandamide, and its synthetic analogue methanandamide, have dual effects. At low concentrations, anandamide selectively activates CB_1 receptors, while at high concentrations it activates excitatory TRPV1 receptors[24]. In pre-contracted strips of rat hepatic artery, rat small mesenteric artery and guinea-pig basilar artery, vasorelaxation induced by high-concentration anandamide is antagonized by the TRPV1 antagonist capsazepine, but not by the CB_1 receptor antagonist SR141716 (0.3 μmol/L)[4]. Further evidence indicates that anandamide not only acts on transfected TRPV1 receptors to produce membrane currents and increase the intracellular Ca^{2+} concentration[4, 32], but also acts on naturally-expressed TRPV1 receptors in neonatal rat dorsal root ganglia to produce membrane currents[33]. Here, we present strong evidence that anandamide selectively activates the CB_1 receptor at low concentrations in small trigeminal ganglion neurons. At high concentrations, anandamide activates both CB_1 and TRPV1 receptors, inhibiting I_{HVA}. To confirm that high-concentration anandamide inhibited I_{HVA} *via* TRPV1 receptor activation, we compared the effects of high-concentration anandamide and the TRPV1 agonist capsaicin. We found that the inhibition induced by high-concentration anandamide and by capsaicin shared similar characteristics. First, both inhibited I_{HVA} in a dose-dependent manner and were reversed by the TRPV1 receptor antagonist capsazepine. Second, like capsaicin, high-concentration anandamide induced inward currents in cultured trigeminal ganglion neurons. Similar to capsaicin-induced inward current, the

reversal potential of anandamide-induced current was also around 0 mV. Anandamide had different effects at low and high concentration *via* the activation of different receptors. By comparing the contribution of CB_1 and TRPV1 activation on anandamide-induced increases in intracellular Ca^{2+} concentration, we conclude that anandamide-induced inhibition of high voltage-activated Ca^{2+} channels and an increase in intracellular Ca^{2+} concentration have the same dual effects as activation of the receptor pathway.

Inhibition of high voltage-activated Ca^{2+} channels and modulation of Ca^{2+} influx are important for neuronal activity and neurotransmitter release induced by endocannabinoids. However, evidence also suggests that cannabinoids can couple to G_s [18] and G_q [19] and activate TRPV1 receptors to increase Ca^{2+} influx. In addition, the response of cannabinoids on intracellular Ca^{2+} concentration differs across cell types[34]. To elucidate the complex mechanisms underlying the intracellular Ca^{2+} response, we further tested the effect of anandamide on intracellular Ca^{2+} concentration. We found that anandamide increased intracellular Ca^{2+} and simultaneously inhibited I_{HVA} in the same population of trigeminal ganglion neurons, providing strong evidence that an increase in the intracellular Ca^{2+} concentration is not due to I_{HVA}. We found that anandamide had dual effects on the inhibition of I_{HVA} and elevation of intracellular Ca^{2+} concentration. However, by comparing the contribution of second messenger system, we found that cAMP- and cGMP-dependent protein kinase antagonists both reversed the anandamide-induced increase in intracellular calcium concentration and I_{HVA} inhibition. Application of a protein kinase C antagonist reversed the inhibition of I_{HVA} but the anandamide-induced increase in intracellular Ca^{2+} concentration was not blocked. From this, we can conclude that the increase in intracellular Ca^{2+} concentration and the I_{HVA} inhibition observed with anandamide are separate processes that share the same receptors but differ in intracellular signal transduction pathways.

CB_1 receptor activation by endocannabinoids has been mostly reported to cause depression of neuronal excitability and neurotransmitter release in presynaptic primary neurons[10, 13, 25, 28, 35-36]. Accumulating evidence indicates that cannabinoids may contribute to the potentiation of neurotransmission. Endocannabinoid release potentiates synaptic transmission *via* CB_1 receptor activation and dopamine release in the goldfish Mauthner cell[37]. Moreover, endocannabinoids may potentiate hippocampal synaptic transmission *via* astrocytic CB_1 activation[30]. In the suprachiasmatic nucleus, CB_1 receptor activation can increase excitability of circadian clock neurons[38]. It is widely accepted that CB_1 receptor activation suppresses neurotransmission by inhibiting high voltage-activated Ca^{2+} channels, and decreases Ca^{2+} influx. In contrast to this general hypothesis, we found that endocannabinoids caused elevation of the intracellular Ca^{2+} concentration in trigeminal ganglion neurons, which was triggered by endocannabinoid-evoked inward current around the resting membrane potential (−60 mV). Furthermore, endocannabinoid-induced increase in intracellular Ca^{2+} concentration and decrease of high voltage-activated Ca^{2+} channels were two independent events, which had the same dual effects *via* similar receptor pathways, but differed in the second messenger transduction pathway. Thus, our results suggest that presynaptic endocannabinoid release might potentiate neurotransmission *via* endocannabinoid-evoked current, increased Ca^{2+} influx, and increased intracellular Ca^{2+} concentration.

In summary, anandamide dose-dependently causes an increase in intracellular Ca^{2+} concentration, mediated by Ca^{2+} influx *via* anandamide-evoked currents, but not high voltage-activated Ca^{2+} channels. In the same population of trigeminal ganglion neurons, CB_1 receptor activation-induced inhibition of I_{HVA} and increase in high voltage-activated Ca^{2+} channels are two separate processes that share the same (CB_1) receptors, but differ in signal transduction pathway. Thus, the effects of anandamide on high voltage-activated Ca^{2+} channels ultimately depend on the balance between the increased Ca^{2+} influx *via* anandamide-evoked currents and inhibition of high voltage-activated Ca^{2+} channels, suggesting a complex role of anandamide on inhibitory or excitatory neuromodulation. Contrary to the general hypothesis of endocannabinoid depression on neurotransmission, this study elucidates possible mechanisms underlying endocannabinoid-induced potentiation of neurotransmission *via* Ca^{2+} signaling modulation.

Materials and Methods

Design

A cytological *in vitro* study.

Time and setting

All data were collected at the Departments of Pharmacology and Physiology, Tongji Medical College, *Huazhong University of Science and Technology in* China from September 2003 to April 2008. Data analysis and manuscript writing were performed at Baylor Medical College, USA, from April 2011 to October 2012.

Materials

180 male Sprague-Dawley rats weighing 180–200 g and aged 6–8 weeks were used. All animal protocols were approved by the faculty of Laboratory Animal Science, Huazhong University of Science and Technology (license No. SYXK (E) 2009-0049). All the experiments followed the *Guidance Suggestions for the Care and Use of Laboratory Animals*, formulated by the Ministry of Science and Technology of China[39].

Methods

Cell dissociation

Trigeminal ganglion neurons from Sprague-Dawley rats were cultured as described previously[40]. Briefly, trigeminal ganglia were dissected aseptically and washed with cold (4°C) modified Hank's balanced salt solution containing NaCl 130 mmol/L, KCl 5 mmol/L, KH_2PO_4 0.3 mmol/L, $NaHCO_3$ 4.0 mmol/L, NaH_2PO_4 0.3 mmol/L, D-glucose 5.6 mmol/L, and ethylene glycol bis(alpha-aminoethyl ether)-N, N′-tetraacetic acid 10 mmol/L, hydroxyethyl piperazine ethanesulfonic acid 10 mmol/L, at pH 7.4. The ganglia were chopped into small pieces, and then incubated in 3 mL modified Hank's solution with 0.1% collagenase (type XI–S)

for 20–40 minutes at 37°C. Individual cells were dissociated by triturating them through a fire-polished glass pipette, followed by incubating with 10 μg/mL DNase I (type lV) in F12 medium (Life Technologies, Gaithersburg, MD, USA) for 10 minutes at 37°C, before centrifuging for 5 minutes at 1,000 r/min. After centrifuging three times, the cells were cultured in F12 supplemented with 10% fetal bovine serum. The cells were planted on poly-D-lysine pre-coated glass coverslips (15 mm diameter) and cultured no more than 12 hours at 37°C in a water saturated atmosphere with 5% CO_2.

Patch-clamp recording

The cells were placed in a recording chamber mounted on an inverted microscope (Leica Inc., Solms, Germany) and perfused with extracellular solution at room temperature (21–22°C). Whole-cell patch-clamp experiments were carried out using an Axopatch 200B amplifier (Axon Instruments, Foster City, CA, USA) and the output was digitized with a Digidata 1332A converter (Axon Instruments) and program pCLAMP 9.02 (Axon Instruments). Data were acquired at a sampling rate of 2 KHz. Cell membrane capacitance and series resistance were measured and compensated (> 90%). Data obtained from neurons in which uncompensated series resistance resulted in voltage-clamp errors > 5 mV were not taken into further analysis. The cell diameters were measured with a calibrated eyepiece under phase contrast illumination.

The resistance of the microelectrode was 2–4 MΩ when filled with the pipette solution. The microelectrode was made from G85150T-4 glass pipettes (Warner Instruments Inc., Hamden, CT, USA). The external solution contained Choline-Cl 110 mmol/L, TEACl 20 mmol/L, $BaCl_2$ 10 mmol/L, $MgCl_2$ 2.0 mmol/L, hydroxyethyl piperazine ethanesulfonic acid 10 mmol/L, and D-glucose 20 mmol/L, adjusted to pH 7.4 with CsOH. Ba^{2+} was used as the charge carrier when recording I_{HVA}. Ba^{2+} was replaced by Ca^{2+} when recording anandamide-evoked currents. The pipette solution contained CsCl 120 mmol/L, $CaCl_2$ 0.1 mmol/L, $MgCL_2$ 2.0 mmol/L, ethylene glycol bis(alpha-aminoethyl ether)-N, N′-tetraacetic acid 10.0 mmol/L, hydroxyethyl piperazine ethanesulfonic acid 10.0 mmol/L and Tris-ATP 5.0 mmol/L, pH adjusted to 7.2 with CsOH. Small-sized cells were selected to perform the further experiments.

The volume of the recording chamber was about 1 mL and the local superfusion rate was 1 mL/min.

Calcium imaging

Drug-induced changes of high voltage-activated Ca^{2+} channels were measured using a confocal laser scanning imaging system (Fluoview FV500, Olympus, Tokyo, Japan). The trigeminal ganglion cells on glass cover slips were loaded with Fluo 2-AM by incubation with 1–5 μmol/L Fluo 2-AM in standard external solution and were maintained in the dark for 30–40 minutes. The standard external solution contained NaCL 140.0 mmol/L, KCL 5.0 mmol/L, $CaCL_2$ 2.0 mmol/L, $MgCL_2$ 1.0 mmol/L, glucose 10.0 mmol/L and hydroxyethyl piperazine ethanesulfonic acid 10.0 mmol/L, pH adjusted to 7.4 with NaOH. Ca^{2+}-free medium solution was identical except for the 2.0 mmol/L Ca^{2+} and additional 10 mmol/L ethyleneglycol bis(alpha-aminoethyl ether)-N, N′-tetraacetic acid to lower extracellular Ca^{2+} concentration. Small-sized trigeminal ganglion neurons (< 33 μmol/L) were selected to perform the further experiments.

Data analysis

The data were analyzed using pCLAMP 9.02 (Axon Instruments) and Sigmaplot 11.0 software (Systat Software Inc., San Jose, CA, USA). The amplitude of I_{HVA} was calculated as the peak current. Voltage-dependent activation for the study of changes on I_{HVA} was measured by a series of depolarized pulses (450 ms) from −50 mV to +40 mV, stepping by 10 mV with interval time of 5 seconds, at a holding potential of −80 mV. We fitted a Boltzmann function to the voltage-dependent activation curves, that is $G/G_{max}=1/[1+\exp(V_{0.5}-V_m)/k]$, where G_{max} is the maximum conductance, $V_{0.5}$ is the membrane potential at which 50% of activation was observed, and k is the slope of the function. Voltage-dependent inactivation was measured by a two pulse protocol in which the precondition pulses (3 seconds) ranged from −80 to +20 in 10 mV increments; following test pulse (200 millsecords) was +10 mV with an internal time of 6 seconds. The Boltzmann function was also fitted to the h-infinity curve, that is, $I/I_{max}=1/[1+\exp(V_{0.5}-V_m)/k]$, where $V_{0.5}$ is the membrane potential at which 50% of inactivation was observed, and k is the slope of the function. The dose-response curve was fitted by the Hill equation, in which, $I_{peak}=I_{peakmax}/[1+(IC_{50}/C)^n]$, with IC_{50} as the concentration producing 50% inhibition and *n* as the Hill coefficient.

Statistical analysis

Data were presented as mean ± SEM. For all experiments, data were examined for Gaussian distribution first, and then analyzed for statistical significance using the paired or unpaired *t*-test and one-way analysis of variance by using Sigma plot 11.0 software (Systat Software Inc.). A value of $P < 0.05$ was considered statistically significant.

Author contributions: *Liu LJ and Cao XH conceived the study and developed crucial proof-of-concept studies. Zhang Y contributed to data analysis and revised manuscript. Xie H performed calcium imaging. Lei G, Li F and Pan JP performed cell dissociation and data analysis. Liu ZG contributed to revised manuscript. Liu CJ also contributed to revised manuscript and study design. All authors approved the final version of the paper.*

Conflicts of interest: *None declared.*

Peer review: *This study systemically determines how anandamide affects Ca^{2+} signaling and underlying mechanisms in small trigeminal ganglion neurons, via the effects of high voltage-activated Ca^{2+} currents, Ca^{2+} influx and intracellular Ca^{2+} concentration, as well as the underlying mechanisms of which in small trigeminal ganglion neurons. This study will benefit the understanding and development of cannabinoids in clinical practice.*

References

[1] Matsuda LA, Lolait SJ, Brownstein MJ, et al. Structure of a cannabinoid receptor and functional expression of the cloned cDNA. Nature. 1990;346(6284):561-564.

[2] Pertwee RG, Ross RA. Cannabinoid receptors and their ligands. Prostaglandins Leukot Essent Fatty Acids. 2002;66(2-3):101-21.
[3] Van Der Stelt M, Di Marzo V. Endovanilloids. Putative endogenous ligands of transient receptor potential vanilloid 1 channels. Eur J Biochem. 2004;271(10):1827-1834.
[4] Zygmunt PM, Petersson J, Andersson DA, et al. Vanilloid receptors on sensory nerves mediate the vasodilator action of anandamide. Nature. 1999;400(6743):452-457.
[5] Tsumura M, Sobhan U, Muramatsu T, et al. TRPV1-mediated calcium signal couples with cannabinoid receptors and sodium-calcium exchangers in rat odontoblasts. Cell Calcium. 2012;52(2):124-136.
[6] De Petrocellis L, Vellani V, Schiano-Moriello A, et al. Plant-derived cannabinoids modulate the activity of transient receptor potential channels of ankyrin type-1 and melastatin type-8. J Pharmacol Exp Ther. 2008;325(3):1007-1015.
[7] Fisyunov A, Tsintsadze V, Min R, et al. Cannabinoids modulate the P-type high-voltage-activated calcium currents in purkinje neurons. J Neurophysiol. 2006;96(3):1267-1277.
[8] Roberts LA, Ross HR, Connor M. Methanandamide activation of a novel current in mouse trigeminal ganglion sensory neurons in vitro. Neuropharmacology. 2008;54(1):172-180.
[9] van der Stelt M, Di Marzo V. Anandamide as an intracellular messenger regulating ion channel activity. Prostaglandins Other Lipid Mediat. 2005;77(1-4):111-122.
[10] Kim HI, Kim TH, Shin YK, et al. Anandamide suppression of Na^+ currents in rat dorsal root ganglion neurons. Brain Res. 2005; 1062(1-2):39-47.
[11] Howlett AC, Qualy JM, Khachatrian LL. Involvement of Gi in the inhibition of adenylate cyclase by cannabimimetic drugs. Mol Pharmacol. 1986;29(3):307-313.
[12] Guo J, Ikeda SR. Endocannabinoids modulate N-type calcium channels and G-protein-coupled inwardly rectifying potassium channels via CB1 cannabinoid receptors heterologously expressed in mammalian neurons. Mol Pharmacol. 2004;65(3):665-674.
[13] Lalonde MR, Jollimore CA, Stevens K, et al. Cannabinoid receptor-mediated inhibition of calcium signaling in rat retinal ganglion cells. Mol Vis. 2006;12:1160-1166.
[14] Twitchell W, Brown S, Mackie K. Cannabinoids inhibit N- and P/Q-type calcium channels in cultured rat hippocampal neurons. J Neurophysiol. 1997;78(1):43-50.
[15] Hampson RE, Mu J, Deadwyler SA. Cannabinoid and kappa opioid receptors reduce potassium K current via activation of G(s) proteins in cultured hippocampal neurons. J Neurophysiol. 2000; 84(5):2356-2364.
[16] Li Q, Ma HJ, Song SL, et al. Effects of anandamide on potassium channels in rat ventricular myocytes: a suppression of I(to) and augmentation of K(ATP) channels. Am J Physiol Cell Physiol. 2012;302(6):C924-930.
[17] Wang W, Zhang K, Yan S, et al. Enhancement of apamin-sensitive medium afterhyperpolarization current by anandamide and its role in excitability control in cultured hippocampal neurons. Neuropharmacology. 2011;60(6):901-909.
[18] Kearn CS, Blake-Palmer K, Daniel E, et al. Concurrent stimulation of cannabinoid CB1 and dopamine D2 receptors enhances heterodimer formation: a mechanism for receptor cross-talk? Mol Pharmacol. 2005;67(5):1697-704.
[19] Lauckner JE, Hille B, Mackie K. The cannabinoid agonist WIN55,212-2 increases intracellular calcium via CB1 receptor coupling to Gq/11 G proteins. Proc Natl Acad Sci U S A. 2005; 102(52):19144-19149.
[20] Szallasi A, Blumberg PM. Vanilloid (Capsaicin) receptors and mechanisms. Pharmacol Rev. 1999;51(2):159-212.
[21] Price TJ, Helesic G, Parghi D, et al. The neuronal distribution of cannabinoid receptor type 1 in the trigeminal ganglion of the rat. Neuroscience. 2003;120(1):155-162.
[22] Freund TF, Katona I, Piomelli D. Role of endogenous cannabinoids in synaptic signaling. Physiol Rev. 2003;83(3):1017-1066.
[23] De Petrocellis L, Bisogno T, Maccarrone M, et al. The activity of anandamide at vanilloid VR1 receptors requires facilitated transport across the cell membrane and is limited by intracellular metabolism. J Biol Chem. 2001;276(16):12856-12863.
[24] Ahluwalia J, Urban L, Bevan S, et al. Anandamide regulates neuropeptide release from capsaicin-sensitive primary sensory neurons by activating both the cannabinoid 1 receptor and the vanilloid receptor 1 in vitro. Eur J Neurosci. 2003;17(12):2611-2618.
[25] Price TJ, Patwardhan A, Akopian AN, et al. Modulation of trigeminal sensory neuron activity by the dual cannabinoid-vanilloid agonists anandamide, N-arachidonoyl-dopamine and arachidonyl-2-chloroethylamide. Br J Pharmacol. 2004;141(7):1118-1130.
[26] Tal M, Devor M. Ectopic discharge in injured nerves: comparison of trigeminal and somatic afferents. Brain Res. 1992;579(1):148-151.
[27] Ahluwalia J, Urban L, Capogna M, et al. Cannabinoid 1 receptors are expressed in nociceptive primary sensory neurons. Neuroscience. 2000;100(4):685-688.
[28] Khasabova IA, Simone DA, Seybold VS. Cannabinoids attenuate depolarization-dependent Ca2+ influx in intermediate-size primary afferent neurons of adult rats. Neuroscience. 2002;115(2):613-625.
[29] Ryan D, Drysdale AJ, Pertwee RG, et al. Differential effects of cannabis extracts and pure plant cannabinoids on hippocampal neurones and glia. Neurosci Lett. 2006;408(3):236-241.
[30] Navarrete M, Araque A. Endocannabinoids potentiate synaptic transmission through stimulation of astrocytes. Neuron. 2010; 68(1):113-126.
[31] Price TJ, Patwardhan A, Akopian AN, et al. Cannabinoid receptor-independent actions of the aminoalkylindole WIN 55,212-2 on trigeminal sensory neurons. Br J Pharmacol. 2004;142(2):257-266.
[32] Lam PM, Hainsworth AH, Smith GD, et al. Activation of recombinant human TRPV1 receptors expressed in SH-SY5Y human neuroblastoma cells increases [Ca(2+)](i), initiates neurotransmitter release and promotes delayed cell death. J Neurochem. 2007; 102(3):801-811.
[33] Evans RM, Scott RH, Ross RA. Multiple actions of anandamide on neonatal rat cultured sensory neurones. Br J Pharmacol. 2004;141(7):1223-1233.
[34] Sugiura T, Kodaka T, Kondo S, et al. 2-Arachidonoylglycerol, a putative endogenous cannabinoid receptor ligand, induces rapid, transient elevation of intracellular free Ca2+ in neuroblastoma x glioma hybrid NG108-15 cells. Biochem Biophys Res Commun. 1996;229(1):58-64.
[35] Morisset V, Ahluwalia J, Nagy I, et al. Possible mechanisms of cannabinoid-induced antinociception in the spinal cord. Eur J Pharmacol. 2001;429(1-3):93-100.
[36] Chevaleyre V, Takahashi KA, Castillo PE. Endocannabinoid-mediated synaptic plasticity in the CNS. Annu Rev Neurosci. 2006; 29:37-76.
[37] Cachope R, Mackie K, Triller A, et al. Potentiation of electrical and chemical synaptic transmission mediated by endocannabinoids. Neuron. 2007;56(6):1034-1047.
[38] Acuna-Goycolea C, Obrietan K, van den Pol AN. Cannabinoids excite circadian clock neurons. J Neurosci. 2010;30(30):10061-10066.
[39] The Ministry of Science and Technology of the People's Republic of China. Guidance Suggestions for the Care and Use of Laboratory Animals. 2006-09-30.
[40] Liu L, Zhu W, Zhang ZS, et al. Nicotine inhibits voltage-dependent sodium channels and sensitizes vanilloid receptors. J Neurophysiol. 2004;91(4):1482-1491.

Copyedited by Slone-Murphy J, Xue T, Pan AH, Wang J, Qiu Y, Li CH, Song LP, Zhao M